Enhanced laser-energy coupling with small-spot distributed phase plates (SG5-650) in OMEGA DT cryogenic target implosions

W. Theobald, D. Cao, R. C. Shah, et al.

Enhanced laser-energy coupling with small-spot distributed phase plates (SG5-650) in OMEGA DT cryogenic target implosions

View Online   Export Citation   CrossMark

W. Theobald,[1,2,a] (iD) D. Cao,[1] R. C. Shah,[1] C. A. Thomas,[1] I. V. Igumenshchev,[1] K. A. Bauer,[1] R. Betti,[1,2,3] M. J. Bonino,[1] E. M. Campbell,[1] A. R. Christopherson,[1,2,b] (iD) K. Churnetski,[1,2] D. H. Edgell,[1] (iD) C. J. Forrest,[1] J. A. Frenje,[4] (iD) M. Gatu Johnson,[4] (iD) V. Yu. Glebov,[1] (iD) V. N. Goncharov,[1] V. Gopalaswamy,[1] (iD) D. R. Harding,[1] S. X. Hu,[1,2] (iD) S. T. Ivancic,[1] D. W. Jacobs-Perkins,[1] (iD) R. T. Janezic,[1] T. Joshi,[1] J. P. Knauer,[1] A. Lees,[1] R. W. Luo,[5] O. M. Mannion,[1,3,c] (iD) F. J. Marshall,[1] (iD) Z. L. Mohamed,[1] S. F. B. Morse,[1] D. Patel,[1] J. L. Peebles,[1] R. D. Petrasso,[4] P. B. Radha,[1] H. G. Rinderknecht,[1] M. J. Rosenberg,[1] S. Sampat,[1] T. C. Sangster,[1] W. T. Shmayda,[1] C. M. Shuldberg,[5] A. Shvydky,[1] C. Sorce,[1] C. Stoeckl,[1] M. D. Wittman,[1] and S. P. Regan[1,2]

AFFILIATIONS

[1]Laboratory for Laser Energetics, University of Rochester, Rochester, New York 14623, USA
[2]Department of Mechanical Engineering, University of Rochester, Rochester, New York 14623, USA
[3]Department of Physics and Astronomy, University of Rochester, Rochester, New York 14623, USA
[4]Plasma Science and Fusion Center, Massachusetts Institute of Technology, Cambridge, Massachusetts 02139, USA
[5]General Atomics, San Diego, California 92121, USA

[a]Author to whom correspondence should be addressed: wthe@lle.rochester.edu
[b]Present address: Lawrence Livermore National Laboratory, Livermore, California 94550, USA.
[c]Present address: Sandia National Laboratories, New Mexico 87123, USA.

ABSTRACT

Cryogenic deuterium–tritium ice target implosions on OMEGA with new small-spot (SG5-650) distributed phase plates (DPPs) achieved an $(11 \pm 4)\%$ increase in energy coupling compared to implosions with larger-spot SG5-850 DPPs by decreasing the ratio of the laser spot diameter to the target diameter from 0.93 to 0.75. The SG5-650 DPPs provide a focus spot size of 674 μm, which is defined as the diameter that encircles 95% of the measured beam energy compared to 834 μm for the SG5-850, which are the standard DPPs in cryogenic target implosions on OMEGA. The hydrodynamic efficiency, defined as the ratio of the kinetic energy in the imploding shell to the laser energy, increased from 4.5% to 5.0% based on radiation-hydrodynamic calculations benchmarked to shell trajectory and bang-time measurements. The higher coupling came with a trade-off of an increased hot-electron production as well as increased hydrodynamic instabilities seeded by a larger mode-10 amplitude from the beam port geometry, both of which may have reduced the fusion neutron production and areal density.

Published under an exclusive license by AIP Publishing. https://doi.org/10.1063/5.0072579

I. INTRODUCTION

Cryogenically layered deuterium–tritium (DT) targets are imploded on the 60-beam, 30-kJ, 351-nm OMEGA laser[1] to study laser direct-drive inertial confinement fusion.[2] The implosions produce hot-spot pressures exceeding 50 Gbar,[3] and recently, a tripling in the neutron yield was achieved through the application of statistical modeling.[4] The goal over the next several years is to optimize those implosions and to demonstrate ignition-relevant implosions that when scaled to 2 MJ of laser energy would enter the burning-plasma regime.[5] A major factor that limits the ablation pressure in direct-drive

implosions is cross-beam energy transfer (CBET).[6] Analysis of radiation-hydrodynamic simulations shows a reduction in the ablation pressure by as much as 40% on OMEGA and up to 60% on National Ignition Facility (NIF)-scale targets, which leads to lower implosion velocity and less shell kinetic energy.[7] One of the CBET mitigation strategies involves using laser illumination with a laser beam spot that is smaller than the target. Experiments with room-temperature plastic-shell targets were performed on OMEGA to test this strategy by varying the target size while keeping the beam spot size fixed.[8] The ratio R of the laser spot diameter to target diameter varied from $R = 1.1$ to 0.5.

A significant increase in the hydrodynamic efficiency for smaller ratios was reported, which was partially caused by smaller refraction losses and partially by reduced CBET losses. Refraction losses are caused by a significant nonzero angle of an incident ray and the radial direction at the beam periphery.

The hydrodynamic efficiency η is defined as the ratio of the kinetic energy of the imploding shell at the end of the acceleration phase and the laser energy, $\eta = \left(\frac{1}{2}mv^2\right)/E_L$, where m is the mass of the unablated shell (determined from simulations), v is the shell velocity (determined from shell trajectory measurements), and E_L is the laser energy. For $R \approx 1$, laser light passing around the target can seed stimulated Brillouin scattering (SBS) in other beams and scatter light out of the central portion of the beam. In addition, a significant beam portion at the outer periphery impinges on the target approaching tangential incidence, which leads to energy losses because of refraction. By reducing R, both CBET and refraction losses are reduced, leading to an enhanced η.

This paper demonstrates improved energy coupling in cryogenic DT-ice target implosions on OMEGA using new smaller-spot (SG5-650) distributed phase plates (DPPs) and standard-size targets with an outer diameter of $\sim$900 μm and $R = 0.75$. In contrast to the previous experiments with CH shells and standard SG5-850 DPPs, these experiments are directly relevant to the cryo program. The SG5-650s allow us to keep standard-size targets, resulting in high-implosion velocity, high-performing implosions. $R = 0.75$ experiments with standard SG5-850 DPPs require targets with a diameter of 1120 μm. Those shells are about 50% more massive for the same DT ice thickness, which significantly lowers the implosion velocity. The primary objective of the SG5-650 implosions was to infer energy coupling by comparing the data from various diagnostics to radiation-hydrodynamic simulations. A secondary objective was to assess the implosion performance based on the measured neutron yield and areal density at stagnation and compare it to similar implosions with the standard SG5-850 DPPs and $R \approx 0.92$–1. The ablation-front shell trajectory, backscattered laser energy, and neutron bang time were found to be consistent with an $\sim$10% increase in energy coupling. The implosion performance was limited by an increase in hot-electron production and increased hydrodynamic instabilities associated with the smaller laser spots. The effects of large-scale (with Legendre modes $\leq$10) laser-imposed nonuniformities were investigated using three-dimensional (3D) hydrodynamic simulations with ASTER, which show that with SG5-650 DPPs, the implosion performance suffers more from illumination nonuniformities than similar implosions with the standard DPPs.[9]

This paper is structured as follows: Sec. II discusses the experimental setup including the measured laser spot profiles, the laser pulse shapes, and the target parameters. Section III presents the experimental data from neutron, optical, and x-ray diagnostics and compares them to hydrodynamic simulations. Section IV summarizes the paper and gives a brief outlook on future work.

II. EXPERIMENTAL SETUP

The experiment was performed in the target chamber of the 60-beam OMEGA (351-nm-wavelength) laser system[1] at the Laboratory for Laser Energetics. The 60 beams were outfitted with small-spot SG5-650 DPPs,[10,11] polarization smoothing,[12] and two-dimensional (2D) smoothing by spectral dispersion (SSD)[13] at 0.3-THz bandwidth and three color cycles.[14,15] The SG5-650 DPPs produce a focus spot with a diameter that
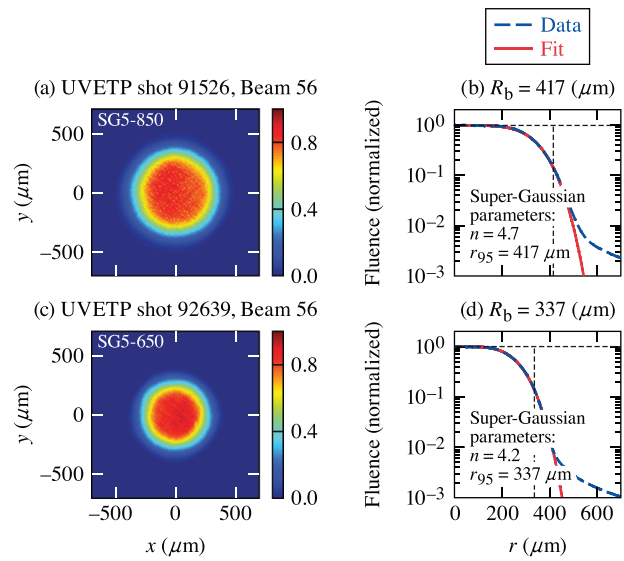

FIG. 1. Measured UV fluence profiles from a UV-equivalent target plane diagnostic (UVETP). Beam 56 was equipped with SG5-850 DPP [(a) and (b)] and with SG5-650 DPP [(c) and (d)]. (b) and (d) Angular averaged radial profiles together with fits from a super-Gaussian function.

is 80% of that of the standard SG5-850 DPPs. Figures 1(a) and 1(c) compare measured UV fluence profiles from both DPPs for beam 56 with a UV-equivalent target-plane diagnostic (UVETP).[16] The images were fitted with an elliptical 2D super-Gaussian function given by $F(x, y) = F_0 \exp[-\{(\frac{x - x_0}{a})^2 + (\frac{y - y_0}{b})^2\}^{\frac{n_{SG}}{2}}]$,[17] where x_0, y_0 are the coordinates of the beam center, n_{SG} is the order, F_0 is the peak fluence, and a and b are the major and minor axes of the ellipse, respectively. The fit also infers the angular variation of the ellipse axes. The x–y directions are those of the rotated coordinate system, in which the direction of the major and minor axes align to the x–y directions. The characteristic radius $R_{1/e} = \sqrt{a \cdot b}$ describes the average radius where the fluence is at the 1/e value of the peak fluence. The two main parameters $R_{1/e}$ and n_{SG} that describe the fluence profiles are $R_{1/e} = 285.6 \pm 1.1\,\mu$m and $n_{SG} = 4.19 \pm 0.14$ for SG5-650 and $R_{1/e} = 362.5 \pm 1.4\,\mu$m and $n_{SG} = 4.74 \pm 0.16$ for SG5-850. The ratio of the major to the minor axis is 1.01, which means that the beam profiles are close to circular. Figures 1(b) and 1(d) present, on a semilogarithmic scale, the radial profiles averaged over the azimuthal angle (blue curves) together with the fits (red curves). The focus spot size is defined as the diameter that encircles 95% of the measured beam energy, which results in $D_{95} = 674 \pm 3\,\mu$m for SG5-650 and $D_{95} = 834 \pm 3\,\mu$m for SG5-850, using the experimental data. The vertical dashed lines indicate the radius connected to the 95% encircled beam energy. An observable difference between data and fit for large radii indicates that the wings of the laser spots are not well described by a super-Gaussian function; however, less than 1% of the laser energy is located in this wing. The UVETP diagnostic samples 4 of the 60 beams. A new diagnostic has been developed—the full-beam-in-tank (FBIT) diagnostic[18]—that directly measures the target-plane beam fluence profile at full energy inside the vacuum chamber with the ultimate goal of characterizing all 60 beams.

The targets consisted of an outer 8-μm-thick plastic ablation layer (deuterated plastic for three implosions and polystyrene for shot 91837) and an inner 68-μm-thick DT ice layer, measured from the b-band image of the ice layer.[19] An excellent layer quality was achieved with a measured b-band ice roughness of 0.77-μm root mean square (rms). The target shells were permeation filled with DT gas 14 days before the experiment. The longer the duration between filling and shot time, the lower the measured neutron yield because of increasing helium-3 buildup inside the capsule and more radiation damage due to the beta decay.[20] The inset in Fig. 2 presents a pie diagram of the target. The outer diameter of the target was 894 $\pm$ 2 μm (the error represents the standard deviation over the measured target diameter of the four targets), providing $R = 0.75$ for SG5-650.

Four DT-ice targets were imploded with two different pulse shapes: a single-picket and a triple-picket pulse shape (see Fig. 2). The laser energy ranged from 26.2 to 27.7 kJ. Those were the types of pulse shapes that were used to create fuel hot-spot pressure in excess of 50 Gbar in previous SG5-850 DPP implosions.[3] The measured power balance between the 60 beams given as rms value was for the pickets 2.1% to 3.6% and for the main drive 3.2% to 3.6%. The *LILAC*-calculated adiabat α for these implosions was $\sim$4.5, where α is defined as the ratio of the minimum fuel pressure in the dense shell and the Fermi-degenerate pressure. The quoted α is the mass-averaged value over the shell radius at the time when the ablation surface reaches 2/3 the initial gas radius corresponding to a convergence ratio of $\sim$1.5.[21]

III. EXPERIMENTAL RESULTS

Table I summarizes the measured laser energy, various measured and simulated stagnation metrics, the measured hard x-ray emission from channel 2 of the hard x-ray detector (HXRD) ($h\nu > 40$ keV, indicator of hot-electron production),[22] the measured neutron bang times t_b, the deconvolved neutron emission duration Δt_b from the neutron temporal diagnostic (NTD),[23,24] the measured asymmetry in ion temperature, and the measured target offset from the requested aim point. Target offsets were generally less than 10 μm except for the
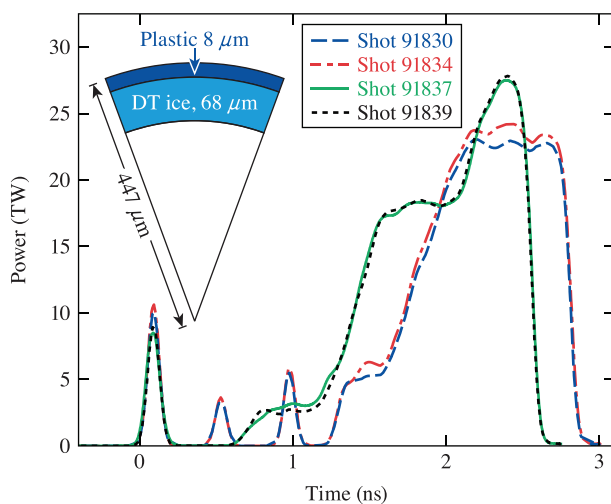
FIG. 2. Measured laser pulse shapes and schematic pie diagram of the target.

E29689J1

last shot. The measured neutron yield is the average value from a Cu activation diagnostic and seven neutron time-of-flight (nTOF) detectors[25] along several lines of sight. The relative standard deviation in the neutron yield measurements is 3.5%. The observed asymmetries in the neutron-averaged ion temperature T_i inferred from the nTOFs, which is defined here as the ratio of the measured maximum and minimum temperatures T_{max}/T_{min}, are generally low. The slightly higher T_{max}/T_{min} in the final shot may be attributed to the 17-μm target offset. A target offset leads to a mode-1 laser-drive asymmetry, resulting in increased T_i asymmetry and a degradation in the neutron yield.[26,27] The statistical model indicates that below a threshold of $T_{max}/T_{min} = 1.14$,[20] there is no measurable degradation from mode 1, and the present implosions are only minimally affected by mode 1.

Table I lists the areal-density (ρR) values that are the error-weighted averages from the magnetic recoil spectrometer (MRS)[28] (forward-scattered neutrons) and the shielded and collimated nTOF[29] in the P7 OMEGA port (backscattered neutrons). The MRS ρR values were higher for all shots than the companion nTOF values. Averaging over the four shots, the MRS reported an $\sim$24% higher value than nTOF. The indicated error represents half of the difference of both values. The MRS probes an annular region of the shell around the P10 port of OMEGA and the nTOF, a circular region around the P6 port with an angular separation of $\sim$65° between both detectors. There is $\sim$20% overlap in the observed surface area between both diagnostics. The ρR difference could be the result of systematic diagnostics errors or might indicate a systematic asymmetry in the shell compression.

Shell trajectories were recorded with the technique described in Ref. 30 for the single-picket-pulse implosions. Figure 3 shows the measured trajectory (red crosses) of the imploding shell for shot 91837 in comparison to simulated trajectories from 1D radiation hydrodynamic simulations with the code *LILAC*[31] assuming SG5-650 DPPs (black curve). *LILAC* includes a 3D ray-trace model taking the exact shape of the focal spot into account, a nonlocal electron thermal conduction model,[32] a CBET model,[6] and first-principles equations of the state.[33] In addition, the blue curve shows the predicted trajectory if the experiment had been performed with SG5-850 DPPs. Figure 4 shows the measured trajectory (red crosses) from a cryogenic DT target implosion (shot 91547) driven by laser beams equipped with SG5-850 DPPs. The measurement is in excellent agreement with the calculated trajectory assuming SG5-850 DPPs in *LILAC* simulation. As expected, the measured shell trajectory in Fig. 3 agrees much better with the simulation for $R = 0.75$ (SG5-650) than for $R = 0.9$ (SG5-850). The simulation with the SG5-850 DPPs shows a delayed shell trajectory. Consequently, the shell is imploding faster with the SG5-650 DPP, indicating a higher hydrodynamic efficiency η. The same conclusion has been obtained from shot 91839—the other single-picket pulse implosion.

The measured neutron bang time and the absorbed laser-energy fraction support the inferred enhanced energy coupling with SG5-650 DPPs (see Fig. 5). For example, for shot 91837, the measured bang time is 2.79 $\pm$ 0.05 ns compared to a predicted bang time of 2.80 ns, and the measured absorption fraction is 0.68 $\pm$ 0.02 compared to a predicted absorption fraction of 0.71. Repeating the simulations with SG5-850 DPPs shows that the predicted bang time is later (2.94 ns), and the absorption fraction is lower (0.65). The same trend is observed for the other three shots. The absorbed laser-energy fraction at the laser wavelength was inferred from the measured backscattered laser

TABLE I. Summary of measured and simulated quantities for the four DT cryogenic target implosions with SG5-650 DPPs. The numbers in parentheses are measurement uncertainties. From left to right, the quantities are the shot number, the total laser energy, the neutron yield, the predicted neutron yield from the statistical model, the yield-over-clean (YOC) defined as the ratio of the measured and 1D simulated neutron yield, the areal density, the ratio of the measured and 1D simulated areal density, the hard x-ray signal from channel 2 of HXRD, the neutron bang time, the neutron emission duration, the ratio of maximum and minimum ion temperature, and the target offset.

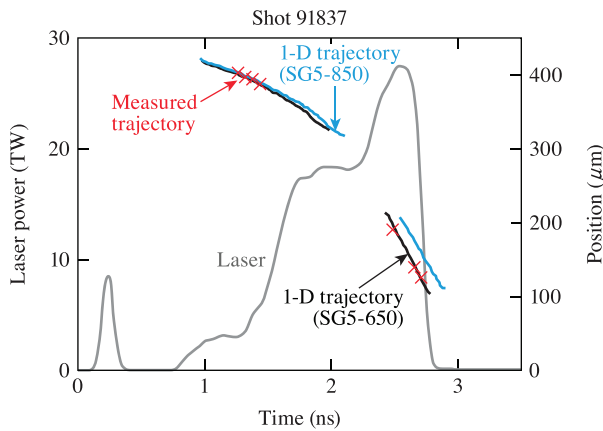| Shot	E_L (kJ)	n-y_{exp}	n-y_{stat}	YOC	ρR (mg/cm^2)	$\rho R/\rho R_{1D}$	HXRD$_2$ (pC)	t_b (ns)	Δt_b (ps)	T_{max}/T_{min}	r_{off} (μm)
91830	26.4	1.72×10^{13}	1.55×10^{13}	19%	120(17)	62%	373(40)	3.03	84	1.10	4
91834	27.7	1.83×10^{13}	1.71×10^{13}	19%	127(3)	63%	406(40)	2.99	85	1.13	7
91837	27.2	2.38×10^{13}	1.95×10^{13}	18%	142(8)	65%	395(40)	2.79	81	1.16	4
91839	27.1	2.16×10^{13}	1.96×10^{13}	14%	132(26)	59%	404(40)	2.78	72	1.21	17

E28755J1

FIG. 3. Measured trajectory (red crosses) of the imploding shell for shot 91837 in comparison to simulated trajectories assuming SG5-650 DPPs (black curve) and SG5-850 DPPs (blue curve). The light gray curve represents the laser pulse.
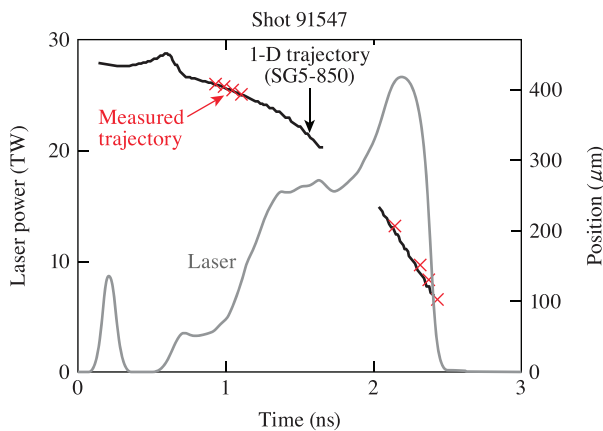

E29690J1

FIG. 4. Measured trajectory (red crosses) of the imploding shell in an experiment with SG5-850 DPPs (shot 91547) in comparison to the simulated trajectory assuming SG5-850 DPPs (black curve). The light gray curve represents the laser pulse. The DT ice thickness was 50 μm, and the target outer radius was 892.4 μm.

energy into two full-aperture backscatter stations (FABSs) and four fixed port scatter calorimeters.[34]

Figure 6 displays the calculated cumulative shell kinetic energy vs time for shot 91837. The energy reaches 1.36 kJ for SG5-650 at bang time and 1.22 kJ for SG5-850, hence an 11.5% increase in the kinetic energy of the imploding shell from the smaller-spot DPP. The calculated hydrodynamic efficiency (η_{calc}) increased from 4.5% with SG5-850 to 5.0% with SG5-650.
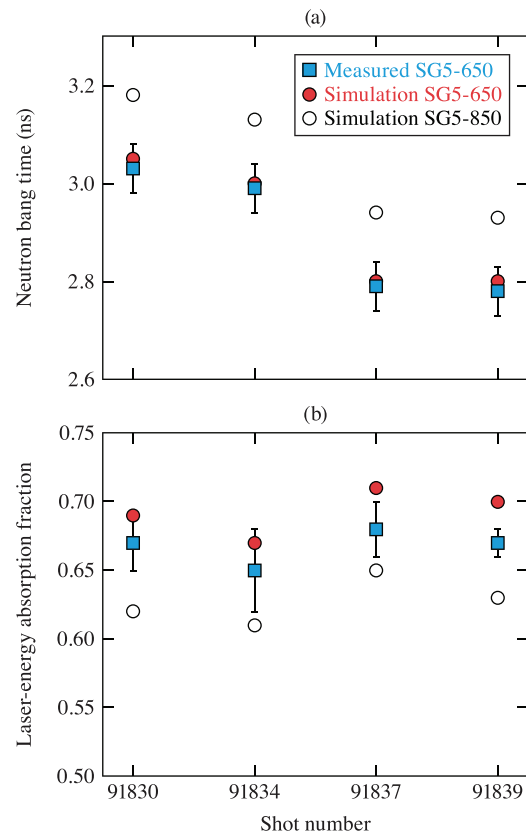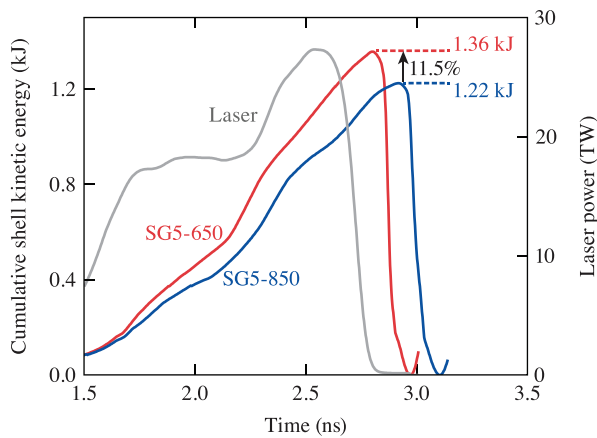

E28759J1

FIG. 5. (a) Measured neutron bang time (blue squares) compared to simulated values with SG5-650 (red circles) and SG5-850 (open circles). (b) Measured energy absorption fraction (blue squares) compared to simulated values with SG5-650 (red circles) and SG5-850 (open circles).

FIG. 6. Calculated cumulative shell kinetic energy vs time for shot 91837. The light gray curve represents the laser pulse.

The experimental coupling efficiencies can be obtained by directly measuring the SG5-650 and the SG5-850 trajectories using the same target and the same laser pulse shape. Unfortunately, no direct comparison to the SG5-650 trajectory experiment is available. An estimate of the experimental increase in η is obtained by considering the time difference Δt between the blue curve in Fig. 3 and the measured trajectory (red crosses) at shell positions at the end of the laser pulse, $\Delta t = t_{850} - t_{\text{exp}}$. Since $\eta \propto v^2$, an incremental increase in velocity provides $\Delta \eta \simeq 2\eta \Delta v / v$, showing that $\Delta \eta$ is proportional to Δv. This only applies where early time features of implosions are identical or very similar. If this is the case, the change in velocity after the acceleration phase results in the shell trajectory reaching a certain radius at a slightly different time. The time difference Δt is proportional to Δv; therefore, the magnitude of $\Delta \eta$ is proportional to Δt: $|\Delta \eta| \propto \Delta t$. For shots 91837 and 91839, the measured Δt yields $\Delta \eta = 4.5 \times 10^{-3}$ and $\Delta \eta = 3.6 \times 10^{-3}$, respectively, by taking a small time difference of 30 ps in the start of acceleration into account. For the current design, shock breakout time is delayed by 30 ps for SG5-850 relative to SG5-650, causing a delay of 30 ps in the SG5-850 trajectory relative to the SG5-650 trajectory. No trajectory measurements are available for shots 91830 and 91834. The experimental uncertainty for $\Delta \eta$ is estimated based on the uncertainty of the absolute timing of the x-ray framing camera, $\delta t = \pm 30 \text{ ps}$,[30] providing $\delta \Delta \eta = \pm 1.2 \times 10^{-3}$. The average value of both shots is $\langle \Delta \eta \rangle = (4.0 \pm 1.2) \times 10^{-3}$ in agreement with the theoretical value of 5.0×10^{-3} within the measurement uncertainty. The relative increase $(\Delta \eta / \eta)_{\text{exp}}$ is, therefore, $(9 \pm 3)\%$.

Similar arguments can be used to infer $\Delta \eta$ from the measured bang times [Fig. 5(a)] relative to the calculated bang time with SG5-850. Knowing that the calculated $(\Delta \eta)_{\text{calc}}$ for shot 91837 is 5.0×10^{-3} and the calculated bang-time shift is 140 ps, the measured bang-time shift of (150 ± 50) ps yields $(\Delta \eta)_{\text{exp}} = (5.5 \pm 1.8) \times 10^{-3}$, again by taking the 30 ps time difference in shock breakout into account. Similar values are obtained for the other three shots since the measured bang-time shifts agree very well with the calculated bang-time shifts. Therefore, the relative increase $(\Delta \eta / \eta)_{\text{exp}}$ is $(11 \pm 4)\%$ for all four shots in agreement with the trajectory measurement and the theoretical value.

From the three diagnostics, the absorbed laser energy fraction is certainly the weakest measurement. The modeling of the scattered light (and therefore the absorption fraction) is complicated by laser-plasma instabilities such as CBET and the two-plasmon-decay (TPD) instability,[35,36] which make it hard to accurately predict the scattered light fraction. In addition, a recent work indicates that the interplay of the current method of polarization smoothing on OMEGA and CBET induces an inherent mode 1 in the laser illumination and not isotropically scattered light,[37] which complicates the absorption fraction inferred from a few local measurements. This uncertainty in modeling the scattered-light fraction and limited diagnostic capability might be the reason why the absorption fraction is slightly overpredicted relative to the measurements.

Although the experiment provides encouraging results from an increased energy coupling, the overall implosion performance (see neutron yield and ρR in Table I) is poorer compared to other high-performing shots with the SG5-850 DPPs.[3,4] Unfortunately, no direct companion SG5-850 shot with the same target and laser pulse shape is available. An example SG5-850 shot (76603) from the 50-Gbar experiment[3] with a 909-μm-OD shell with 53.6 μm of the DT ice thickness but a 1-μm-thicker plastic ablator ($\simeq$ same target mass) and 28.3 kJ of the laser energy achieved a neutron yield of 4.3×10^{13} and $\rho R = (168 \pm 26)$ mg/cm^2. Consequently, the neutron yield is about a factor of 2 higher in shot 76603 compared to the SG5-650 shots. The neutron yield-over-clean (YOC), which is defined as the ratio of the measured yield and the 1D predicted yield from *LILAC* is, on average, $18 \pm 2\%$ for those four SG5-650 shots, while SG5-850 implosions perform better with YOC $= 31 \pm 11\%$. The number for SG5-850 is an average over 99 shots with similar target size but with various pulse shapes and ice thicknesses. The error represents the standard deviation.

The smaller DPP spots limit the implosion performance probably because of increased hydrodynamic instabilities seeded by low- and mid-mode laser illumination nonuniformity. It has been shown with 3D hydrodynamic simulations with the code *ASTER* that SG5-650, $R = 0.75$ implosions are more susceptible to low- and mid-mode perturbations induced by the target offset, beam mispointing, and power balance than similar implosions with SG5-850 and $R = 0.9$.[9] In addition, the beam-port geometry produces, in SG5-650, $R = 0.75$ implosions, a dominant contribution from mid-mode $\ell = 10$. The calculated irradiation nonuniformity (rms-value) from the beam-port geometry alone is 1.1% for SG5-650 and 0.2% for SG5-850, a factor of 5 larger for the smaller-spot DPPs and the same target diameter of 900 μm. Figure 7 shows the hard sphere illumination calculations for the two DPPs using the same scale. This demonstrates significantly enhanced illumination nonuniformity from the beam-port geometry. On shot 91839, we have tried to mitigate the mode $\ell = 10$ nonuniformity by defocusing the laser beams. No significant change in performance was observed, however, relative to companion shot 91837.

A physics-based statistical mapping framework of the OMEGA experimental and simulation databases has been developed[20] that identifies and quantifies the various degradation mechanisms of the neutron yield. The most important degradation mechanism is associated with parameter R, the ratio of the laser spot diameter and target diameter. The mapping framework provides a scaling according to YOC$_R \sim R^{2.97}$.[20] Therefore, the relative YOC of $R = 0.75$ and
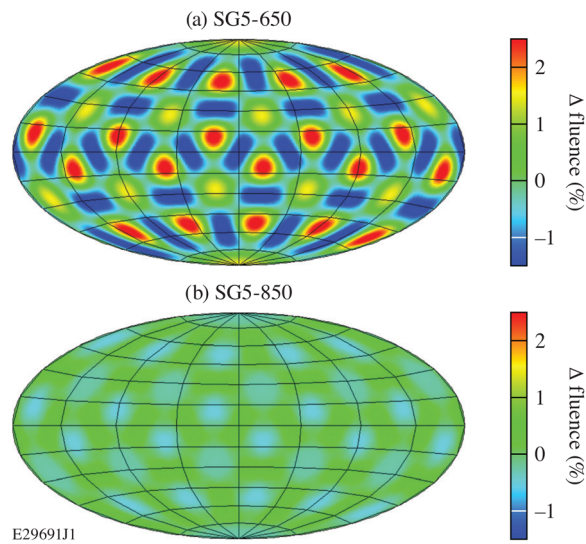
FIG. 7. (a) Hard sphere illumination calculation for SG5-650 DPPs and a target diameter of 900 μm; and (b) the calculation for SG5-850 DPPs.
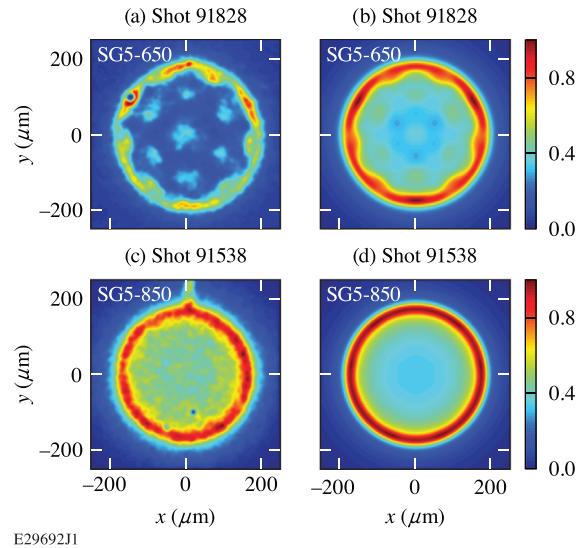

FIG. 8. (a) and (c) Measured gated x-ray images at the end of the acceleration phase with SG5-650 and SG5-850 DPPs; (b) and (d) images from 3D simulations with the code *ASTER*.[9] These images are from plastic-shell implosions taken as companion shots of the DT cryo target implosions.

$R = 0.93$ implosions is expected to degrade by about a factor of 2: $\text{YOC}_{0.75}/\text{YOC}_{0.93} = (0.75/0.93)^{2.97} \approx 0.53$. The statistical model-predicted neutron yields for the $R = 0.75$ shots taking all the different degradation mechanisms into account are given in the fourth column of Table I. The predicted values are slightly lower than the measured neutron yields. The current understanding is that due to the large number of generated hot electrons, those shots are harder to predict.

Further experimental evidence of an increased illumination non-uniformity comes from measured gated x-ray images at the end of the acceleration phase,[30] which show a nonuniform emission pattern for SG5-650 in contrast to a more-uniform emission pattern with SG5-850 (see Fig. 8). Figure 8(a) shows the measured gated x-ray image with SG5-650. The image reveals a regular modal structure along the limb-brightened periphery at the ablation surface of the imploded shell and a regular pattern of seven bright spots in the center, one of which is located in the center and the others arranged on a regular hexagonal pattern on a circle with a radius of ∼150 μm. The convergence ratio of the shell was 2.6 at the time of the measurement. Three-dimensional simulations with the radiation-hydrodynamic code *ASTER*[9] qualitatively reproduce this emission pattern (the modal structure in periphery and bright spots) in the image in Fig. 8(b). In contrast, Figs. 8(c) and 8(d) demonstrate a much more uniform emission with SG5-850 from the measured and simulated images. These two shots (91828, 91538) were performed with room-temperature CH targets in a sequence of preparation shots for cryogenic target implosions in order to optimize the laser pulse shape. This pattern is not observable in the DT cyro target implosions because of a much weaker x-ray emission from the lower-atomic-number material. Shot 91828 with SG5-650 imploded a 27-μm-thick CH shell with an outer diameter of 905 μm and filled with D_2 gas with a pressure of 3 atm. The room-temperature targets were coated with 100 nm of Al for gas retention. The same triple-picket-pulse shape as used for cryo target implosion 91830 (blue curve in Fig. 2) with $E_L = 26.2$ kJ imploded the capsule. Shot 91538

with SG5-850 imploded a 20-μm-thick CH shell with an outer diameter of 864 μm and filled with D_2 gas with a pressure of 16 atm. A single-picket-pulse shape with $E_L = 27.2$ kJ imploded the capsule. The pulse is similar to the single-picket-pulse shape shown in Fig. 2.

The observed modulations in the x-ray emission stem from mass density and temperature modulations in the CH plasma at the ablation region. The modulations are a fingerprint of the irradiation nonuniformity from the beam-port geometry, which becomes visible only when using small-spot DPPs ($R = 0.75$) and CH shell implosions at the end of the acceleration phase. This provides sufficient shell convergence, while the plasma is still hot enough to create observable x-ray emission. A more quantitative analysis of the observed pattern in x-ray emission is outside the scope of this work and will be reported in a forthcoming publication.[38]

SG5-650 implosions also result in lower ρR's than comparable SG5-850 implosions. The degree of compression, which is expressed by the ratio of the measured ρR and the *LILAC*-calculated ρR_{1D}, reaches only $\rho R/\rho R_{1D} = 63 \pm 2\%$, while similar SG5-850 implosions produce close to ∼90%.[3,4] The lower compression might be related to a higher hot-electron preheat level in these implosions. The signals from the HXRD[22] are higher than comparable SG5-850 DT cryogenic implosions. The HXRD signals (see Table I, column 8) are comparable in magnitude for both single- and triple-picket pulses. A direct comparison using the same room-temperature target (20-μm-thick CH shell, 875-μm outer diameter, 16 atm of D_2 gas fill) and the same pulse shape (1-ns square pulse with $E_L = 22.7$ kJ) reveals that the SG5-650 produces a factor of ∼2 more hard x rays ($h\nu > 20$ keV) in all four channels of the HXRD. The explanation is that while SG5-650 DPPs reduce CBET and refraction losses and improve η, this also leads to an increase in the laser intensity at the quarter-critical density ($n_c/4$). Laser-plasma instabilities generate a hot-electron population at this location, predominately through the TPD instability[35] for the plasma

conditions encountered in OMEGA implosions. The hot-electron production from TPD scales with laser intensity at $n_c/4$ for a fixed electron temperature and density scale length. Consequently, higher hard x-ray emission from the target indicates more hot electrons slowing down in the target, which might raise the entropy in the compressed shell.

Experiments with SG5-850 revealed that hot-electron energy deposition into the stagnated DT layer results in an areal-density degradation of ~10%–20%.[39] Based on a factor of ~2 higher hard x-ray signal in similar cryogenic DT target implosions with SG5-650, it is reasonable to assume that the hot-electron deposition into the stagnated DT layer also increases, which should result in an areal-density degradation of more than 20%. The observed ρR degradation is ~40%, indicating that to some degree the increased level of preheat in the compressed shell is responsible for this degradation in compression. A follow-up experiment successfully achieved an improved compression in cryogenic DT target implosions with SG5-650 by reducing the laser intensity. The hard x-ray signal was reduced by a factor of ~4 and the degree of compression improved to up to $\rho R/\rho R_{1D} \sim 85\%$ but not to 100%, indicating that other factors, such as hydrodynamic instabilities, might also play a role in the areal-density degradation. The details of the hot-electron preheat scan and a quantitative analysis of the hot-electron preheat for the SG5-650 implosions will be discussed in a forthcoming paper.[40]

IV. CONCLUSIONS

In conclusion, the ratio of the laser far-field spot diameter to the target diameter has been reduced in an attempt to mitigate cross-beam energy transfer and refraction losses and to improve energy coupling in DT cryogenic target implosions. The 60 OMEGA beams were outfitted with new smaller-spot (SG5-650) distributed phase plates (DPPs) that produce a laser spot that is 80% of that of the standard SG5-850 DPPs. The ablation-front trajectory, the backscattered laser energy, and the neutron bang time were found to be consistent with an ~10% increase in energy coupling. However, an increase in hot-electron production was observed, and evidence was seen in x-ray framing-camera images for increased hydrodynamic instabilities associated with the smaller DPP spots, limiting the implosion performance. Further studies are required on how to maintain the improved energy coupling while mitigating preheat and hydrodynamic instabilities. Future experiments with SG5-650 DPPs will use Si-layered capsules to mitigate hot-electron preheat. The SG5-650 DPPs will also be used to explore experimentally the concept of hydrodynamic scaling.[41] The target size will be reduced to 80% of the size of the best-performing cryogenic DT targets,[4] and the laser drive will be scaled down according to hydrodynamic similarity while keeping the ratio of the laser-spot diameter and target diameter fixed.

ACKNOWLEDGMENTS

AUTHOR DECLARATIONS
Conflict of Interest

The authors have no conflicts of interest to disclose.

DATA AVAILABILITY

The data that support the findings of this study are available from the corresponding author upon reasonable request.

REFERENCES

[1]T. R. Boehly, D. L. Brown, R. S. Craxton, R. L. Keck, J. P. Knauer, J. H. Kelly, T. J. Kessler, S. A. Kumpan, S. J. Loucks, S. A. Letzring, F. J. Marshall, R. L. McCrory, S. F. B. Morse, W. Seka, J. M. Soures, and C. P. Verdon, "Initial performance results of the OMEGA laser system," Opt. Commun. **133**, 495 (1997).

[2]R. S. Craxton, K. S. Anderson, T. R. Boehly, V. N. Goncharov, D. R. Harding, J. P. Knauer, R. L. McCrory, P. W. McKenty, D. D. Meyerhofer, J. F. Myatt, A. J. Schmitt, J. D. Sethian, R. W. Short, S. Skupsky, W. Theobald, W. L. Kruer, K. Tanaka, R. Betti, T. J. B. Collins, J. A. Delettrez, S. X. Hu, J. A. Marozas, A. V. Maximov, D. T. Michel, P. B. Radha, S. P. Regan, T. C. Sangster, W. Seka, A. A. Solodov, J. M. Soures, C. Stoeckl, and J. D. Zuegel, "Direct-drive inertial confinement fusion: A review," Phys. Plasmas **22**, 110501 (2015).

[3]S. P. Regan, V. N. Goncharov, I. V. Igumenshchev, T. C. Sangster, R. Betti, A. Bose, T. R. Boehly, M. J. Bonino, E. M. Campbell, D. Cao, T. J. B. Collins, R. S. Craxton, A. K. Davis, J. A. Delettrez, D. H. Edgell, R. Epstein, C. J. Forrest, J. A. Frenje, D. H. Froula, M. Gatu Johnson, V. Yu. Glebov, D. R. Harding, M. Hohenberger, S. X. Hu, D. Jacobs-Perkins, R. T. Janezic, M. Karasik, R. L. Keck, J. H. Kelly, T. J. Kessler, J. P. Knauer, T. Z. Kosc, S. J. Loucks, J. A. Marozas, F. J. Marshall, R. L. McCrory, P. W. McKenty, D. D. Meyerhofer, D. T. Michel, J. F. Myatt, S. P. Obenschain, R. D. Petrasso, R. B. Radha, B. Rice, M. Rosenberg, A. J. Schmitt, M. J. Schmitt, W. Seka, W. T. Shmayda, M. J. Shoup III, A. Shvydky, S. Skupsky, A. A. Solodov, C. Stoeckl, W. Theobald, J. Ulreich, M. D. Wittman, K. M. Woo, B. Yaakobi, and J. D. Zuegel, "Demonstration of Fuel hot-spot pressure in excess of 50 Gbar for direct-drive, layered deuterium-tritium implosions on OMEGA," Phys. Rev. Lett. **117**, 025001 (2016); "Erratum," **117**, 059903(E) (2016).

[4]V. Gopalaswamy, R. Betti, J. P. Knauer, N. Luciani, D. Patel, K. M. Woo, A. Bose, I. V. Igumenshchev, E. M. Campbell, K. S. Anderson, K. A. Bauer, M. J. Bonino, D. Cao, A. R. Christopherson, G. W. Collins, T. J. B. Collins, J. R. Davies, J. A. Delettrez, D. H. Edgell, R. Epstein, C. J. Forrest, D. H. Froula, V. Yu. Glebov, V. N. Goncharov, D. R. Harding, S. X. Hu, D. W. Jacobs-Perkins, R. T. Janezic, J. H. Kelly, O. M. Mannion, F. J. Marshall, D. T. Michel, S. Miller, S. F. B. Morse, J. P. Palastro, J. Peebles, P. B. Radha, S. P. Regan, S. Sampat, T. C. Sangster, A. B. Sefkow, W. Seka, R. C. Shah, W. T. Shmayda, A. Shvydky, C. Stoeckl, A. A. Solodov, W. Theobald, J. D. Zuegel, M. Gatu Johnson, R. D. Petrasso, C. K. Li, and J. A. Frenje, "Tripled yield in direct-drive laser fusion through statistical modelling," Nature **565**, 581 (2019).

[5]O. A. Hurricane, P. T. Springer, P. K. Patel, D. A. Callahan, K. Baker, D. T. Casey, L. Divol, T. Döppner, D. E. Hinkel, M. Hohenberger, L. F. Berzak Hopkins, C. Jarrott, A. Kritcher, S. Le Pape, S. Maclaren, L. Masse, A. Pak, J. Ralph, C. Thomas, P. Volegov, and A. Zylstra, "Approaching a burning plasma on the NIF," Phys. Plasmas **26**, 052704 (2019).

[6]I. V. Igumenshchev, D. H. Edgell, V. N. Goncharov, J. A. Delettrez, A. V. Maximov, J. F. Myatt, W. Seka, A. Shvydky, S. Skupsky, and C. Stoeckl,

"Crossed-beam energy transfer in implosion experiments on OMEGA," Phys. Plasmas **17**, 122708 (2010).

[7] V. N. Goncharov, S. P. Regan, T. C. Sangster, R. Betti, T. R. Boehly, E. M. Campbell, J. A. Delettrez, D. H. Edgell, R. Epstein, C. J. Forrest, D. H. Froula, V. Yu. Glebov, D. R. Harding, S. X. Hu, I. V. Igumenshchev, F. J. Marshall, R. L. McCrory, D. T. Michel, J. F. Myatt, P. B. Radha, W. Seka, A. Shvydky, C. Stoeckl, W. Theobald, B. Yaakobi, and M. Gatu Johnson, "Demonstrating ignition hydrodynamic equivalence in direct-drive cryogenic implosions on OMEGA," J. Phys.: Conf. Ser. **717**, 012008 (2016).

[8] D. H. Froula, I. V. Igumenshchev, D. T. Michel, D. H. Edgell, R. Follett, V. Yu. Glebov, V. N. Goncharov, J. Kwiatkowski, F. J. Marshall, P. B. Radha, W. Seka, C. Sorce, S. Stagnitto, C. Stoeckl, and T. C. Sangster, "Increasing hydrodynamic efficiency by reducing cross-beam energy transfer in direct-drive-implosion experiments," Phys. Rev. Lett. **108**, 125003 (2012).

[9] I. V. Igumenshchev, V. N. Goncharov, F. J. Marshall, J. P. Knauer, E. M. Campbell, C. J. Forrest, D. H. Froula, V. Yu. Glebov, R. L. McCrory, S. P. Regan, T. C. Sangster, S. Skupsky, and C. Stoeckl, "Three-dimensional modeling of direct-drive cryogenic implosions on OMEGA," Phys. Plasmas **23**, 052702 (2016).

[10] Y. Kato, K. Mima, N. Miyanaga, S. Arinaga, Y. Kitagawa, M. Nakatsuka, and C. Yamanaka, "Random phasing of high-power lasers for uniform target acceleration and plasma-instability suppression," Phys. Rev. Lett. **53**, 1057 (1984).

[11] T. J. Kessler, Y. Lin, J. J. Armstrong, and B. Velazquez, "Phase conversion of lasers with low-loss distributed phase plates," Proc. SPIE **1870**, 95 (1993).

[12] J. E. Rothenberg, "Polarization beam smoothing for inertial confinement fusion," J. Appl. Phys. **87**, 3654 (2000).

[13] S. Skupsky, R. W. Short, T. Kessler, R. S. Craxton, S. Letzring, and J. M. Soures, "Improved laser-beam uniformity using the angular dispersion of frequency-modulated light," J. Appl. Phys. **66**, 3456 (1989).

[14] Laboratory for Laser Energetics, "Broadband beam smoothing on OMEGA with two-dimensional smoothing by spectral dispersion," LLE Review Quarterly Report, LLE Document No. DOE/SF/19460-321(1999).

[15] S. P. Regan, J. A. Marozas, R. S. Craxton, J. H. Kelly, W. R. Donaldson, P. A. Jaanimagi, D. Jacobs-Perkins, R. L. Keck, T. J. Kessler, D. D. Meyerhofer, T. C. Sangster, W. Seka, V. A. Smalyuk, S. Skupsky, and J. D. Zuegel, "Performance of 1-THz-bandwidth, two-dimensional smoothing by spectral dispersion and polarization smoothing of high-power, solid-state laser beams," J. Opt. Soc. Am. B **22**, 998 (2005).

[16] S. P. Regan, J. A. Marozas, J. H. Kelly, T. R. Boehly, W. R. Donaldson, P. A. Jaanimagi, R. L. Keck, T. J. Kessler, D. D. Meyerhofer, W. Seka, S. Skupsky, and V. A. Smalyuk, "Experimental investigation of smoothing by spectral dispersion," J. Opt. Soc. Am. B **17**, 1483 (2000).

[17] R. A. Forties and F. J. Marshall, "In situ characterization of high-intensity laser beams on OMEGA," Rev. Sci. Instrum. **76**, 073505 (2005).

[18] K. A. Bauer, M. Heimbueger, J. Kwiatkowski, S. Sampat, L. J. Waxer, E. C. Cost, J. H. Kelly, V. Kobilansky, S. F. B. Morse, D. Nelson, D. Weiner, G. Weselak, and J. Zou, "Optical characterization of the on-target OMEGA focal spot at high energy using the full-beam in-tank diagnostic," J. Opt. Soc. Am. B **59**, 7994 (2020).

[19] D. H. Edgell, W. Seka, R. S. Craxton, L. M. Elasky, D. R. Harding, R. L. Keck, L. D. Lund, and M. D. Wittman, "Characterization of cryogenic direct-drive ICF targets during layering studies and just prior to shot time," J. Phys. IV **133**, 903 (2006).

[20] A. Lees, R. Betti, J. P. Knauer, V. Gopalaswamy, D. Patel, K. M. Woo, K. S. Anderson, E. M. Campbell, D. Cao, J. Carroll-Nellenback, R. Epstein, C. Forrest, V. N. Goncharov, D. R. Harding, S. X. Hu, I. V. Igumenshchev, R. T. Janezic, O. M. Mannion, P. B. Radha, S. P. Regan, A. Shvydky, R. C. Shah, W. T. Shmayda, C. Stoeckl, W. Theobald, and C. A. Thomas, "Experimentally inferred fusion yield dependencies in OMEGA inertial confinement fusion implosions," Phys. Rev. Lett. **127**, 105001 (2021).

[21] V. N. Goncharov, J. P. Knauer, P. W. McKenty, P. B. Radha, T. C. Sangster, S. Skupsky, R. Betti, R. L. McCrory, and D. D. Meyerhofer, "Improved performance of direct-drive inertial confinement fusion target designs with adiabat shaping using an intensity picket," Phys. Plasmas **10**, 1906 (2003).

[22] C. Stoeckl, V. Yu. Glebov, D. D. Meyerhofer, W. Seka, B. Yaakobi, R. P. J. Town, and J. D. Zuegel, "Hard x-ray detectors for OMEGA and NIF," Rev. Sci. Instrum. **72**, 1197 (2001).

[23] R. A. Lerche, D. W. Phillion, and G. L. Tietbohl, "25 ps neutron detector for measuring ICF target burn history," Rev. Sci. Instrum. **66**, 933 (1995).

[24] C. Stoeckl, R. Boni, F. Ehrne, C. J. Forrest, V. Yu. Glebov, J. Katz, D. J. Lonobile, J. Magoon, S. P. Regan, M. J. Shoup III, A. Sorce, C. Sorce, T. C. Sangster, and D. Weiner, "Neutron temporal diagnostic for high-yield deuterium–tritium cryogenic implosions on OMEGA," Rev. Sci. Instrum. **87**, 053501 (2016).

[25] V. Yu. Glebov, C. Stoeckl, T. C. Sangster, S. Roberts, G. J. Schmid, R. A. Lerche, and M. J. Moran, "Prototypes of National Ignition Facility neutron time-of-flight detectors tested on OMEGA," Rev. Sci. Instrum. **75**, 3559 (2004).

[26] B. K. Spears, M. J. Edwards, S. Hatchett, J. Kilkenny, J. Knauer, A. Kritcher, J. Lindl, D. Munro, P. Patel, H. F. Robey, and R. P. J. Town, "Mode 1 drive asymmetry in inertial confinement fusion implosions on the National Ignition Facility," Phys. Plasmas **21**, 042702 (2014).

[27] O. M. Mannion, I. V. Igumenshchev, K. S. Anderson, R. Betti, E. M. Campbell, D. Cao, C. J. Forrest, M. Gatu Johnson, V. Yu. Glebov, V. N. Goncharov, V. Gopalaswamy, S. T. Ivancic, D. W. Jacobs-Perkins, A. Kalb, J. P. Knauer, J. Kwiatkowski, A. Lees, F. J. Marshall, M. Michalko, Z. L. Mohamed, D. Patel, H. G. Rinderknecht, R. C. Shah, C. Stoeckl, W. Theobald, K. M. Woo, and S. P. Regan, "Mitigation of mode-one asymmetry in laser-direct-drive inertial confinement fusion implosions," Phys. Plasmas **28**, 042701 (2021).

[28] J. A. Frenje, D. T. Casey, C. K. Li, F. H. Séguin, R. D. Petrasso, V. Yu. Glebov, P. B. Radha, T. C. Sangster, D. D. Meyerhofer, S. P. Hatchett, S. W. Haan, C. J. Cerjan, O. L. Landen, K. A. Fletcher, and R. J. Leeper, "Probing high areal-density cryogenic deuterium-tritium implosions using downscattered neutron spectra measured by the magnetic recoil spectrometer," Phys. Plasmas **17**, 056311 (2010).

[29] C. J. Forrest, P. B. Radha, V. Yu. Glebov, V. N. Goncharov, J. P. Knauer, A. Pruyne, M. Romanofsky, T. C. Sangster, M. J. Shoup, C. Stoeckl, D. T. Casey, M. Gatu Johnson, and S. Gardner, "High-resolution spectroscopy used to measure inertial confinement fusion neutron spectra on Omega," Rev. Sci. Instrum. **83**, 10D919 (2012).

[30] D. T. Michel, C. Sorce, R. Epstein, N. Whiting, I. V. Igumenshchev, R. Jungquist, and D. H. Froula, "Shell trajectory measurements from direct-drive implosion experiments," Rev. Sci. Instrum. **83**, 10E530 (2012).

[31] J. Delettrez, R. Epstein, M. C. Richardson, P. A. Jaanimagi, and B. L. Henke, "Effect of laser illumination nonuniformity on the analysis of time-resolved x-ray measurements in uv spherical transport experiments," Phys. Rev. A **36**, 3926 (1987).

[32] V. N. Goncharov, O. V. Gotchev, E. Vianello, T. R. Boehly, J. P. Knauer, P. W. McKenty, P. B. Radha, S. P. Regan, T. C. Sangster, S. Skupsky, V. A. Smalyuk, R. Betti, R. L. McCrory, D. D. Meyerhofer, and C. Cherfils-Clérouin, "Early stage of implosion in inertial confinement fusion: Shock timing and perturbation evolution," Phys. Plasmas **13**, 012702 (2006).

[33] S. X. Hu, L. A. Collins, V. N. Goncharov, J. D. Kress, R. L. McCrory, and S. Skupsky, "First-principles equation of state of polystyrene and its effect on inertial confinement fusion implosions," Phys. Rev. E **92**, 043104 (2015).

[34] W. Seka, D. H. Edgell, J. P. Knauer, J. F. Myatt, A. V. Maximov, R. W. Short, T. C. Sangster, C. Stoeckl, R. E. Bahr, R. S. Craxton, J. A. Delettrez, V. N. Goncharov, I. V. Igumenshchev, and D. Shvarts, "Time-resolved absorption in cryogenic and room-temperature direct-drive implosions," Phys. Plasmas **15**, 056312 (2006).

[35] A. Simon, R. W. Short, E. A. Williams, and T. Dewandre, "On the inhomogeneous two plasmon instability," Phys. Fluids **26**, 3107 (1983).

[36] D. Turnbull, A. V. Maximov, D. H. Edgell, W. Seka, R. K. Follett, J. P. Palastro, D. Cao, V. N. Goncharov, C. Stoeckl, and D. H. Froula, "Anomalous absorption by the two-plasmon decay instability," Phys. Rev. Lett. **124**, 185001 (2020).

[37] D. H. Edgell, P. B. Radha, J. Katz, A. Shvydky, D. Turnbull, and D. H. Froula, "Nonuniform absorption and scattered light in direct-drive implosions driven by polarization smoothing," Phys. Rev. Lett. **127**, 075001 (2021).

[38] T. Joshi, R. Shah, W. Theobald, I. Igumenshchev, D. Cao, J. Balatazar, and S. Regan, "Quantitative analysis of modulations observed in x-ray self-emission images of OMEGA direct-drive inertial confinement fusion implosions," Phys. Plasmas (to be published).

[39]A. R. Christopherson, R. Betti, C. J. Forrest, J. Howard, W. Theobald, J. Delettrez, M. J. Rosenberg, A. Solodov, C. Stoeckl, D. Patel, V. Gopalaswamy, D. Cao, J. Peebles, D. Edgell, W. Seka, R. Epstein, M. S. Wei, M. Gatu Johnson, R. Simpson, S. P. Regan, and E. M. Campbell, "Direct measurements of DT fuel preheat from hot electrons in direct drive inertial confinement fusion," Phys. Rev. Lett. **127**, 055001 (2021).

[40]D. Cao, W. Theobald, M. J. Rosenberg, D. Patel, A. R. Christopherson, C. Stoeckl, S. P. Regan, R. Betti, P. B. Radha, and V. Goncharov, "Hot-electron preheat scan in layered, direct-drive inertial confinement fusion implosions at OMEGA," Phys. Plasmas (to be published).

[41]R. Nora, R. Betti, K. S. Anderson, A. Shvydky, A. Bose, K. M. Woo, A. R. Christopherson, J. A. Marozas, T. J. B. Collins, P. B. Radha, S. X. Hu, R. Epstein, F. J. Marshall, R. L. McCrory, T. C. Sangster, and D. D. Meyerhofer, "Theory of hydro-equivalent ignition for inertial fusion and its applications to OMEGA and the National Ignition Facility," Phys. Plasmas **21**, 056316 (2014).